

Rock mechanics and wellbore stability in Dongfang 1-1 Gas Field in South China Sea

Chuanliang Yan^{*1,2}, Jingen Deng², Yuanfang Cheng¹,
Xinjiang Yan³, Junliang Yuan³ and Fucheng Deng⁴

¹ School of Petroleum Engineering, China University of Petroleum (Huadong), Qingdao, 266580, China

² State Key Laboratory of Petroleum Resources and Prospecting,
China University of Petroleum, Beijing, 102249, China

³ CNOOC Research Institute, Beijing, 100027, China

⁴ Yangtze University, Jingzhou, 434023, China

(Received May 16, 2016, Revised October 19, 2016, Accepted January 12, 2017)

Abstract. Thermal effect has great influence on wellbore stability in Dongfang 1-1 (DF 1-1) gas field, a reservoir with high-temperature and high-pressure. In order to analyze the wellbore stability in DF1-1 gas field, the variation of temperature field after drilling was analyzed. In addition, the effect of temperature changing on formation strength and the thermal expansion coefficients of formation were tested. On this basis, a wellbore stability model considering thermal effect was developed and the thermal effect on fracture pressure and collapse pressure was analyzed. One of the main challenges in this gas field is the decreasing temperature of the wellbore will reduce fracture pressure substantially, resulting in the drilling fluid leakage. If the drilling fluid density was reduced, kick or blowout may happen. Therefore, the key of safe drilling in DF1-1 gas field is to predict the fracture pressure accurately.

Keywords: computing model of temperature field; rock mechanical characteristic; thermal effect; mud circulation; wellbore stability; Dongfang 1-1 gas field; high temperature high pressure

1. Introduction

Dongfang 1-1 (DF1-1) gas field is the largest offshore gas field in China (Jiang *et al.* 2012). Its gas-bearing area covered over 300 km², with the geological reserves more than one hundred billion cubic meters. The field was put into production in 2003, with an annual gas production of 2.4×10⁹ m³. Bottom hole temperature data indicate that the DF1-1 gas field has a relatively uniform thermal regime, with the current geothermal gradient averaging about 4.67°C/100m (Wang and Huang 2008). In DF1-1 gas field, the highest pore pressure of the reservoir was more than 2.0 SG. The characteristic of high temperature and high pressure brings about lots of problems in drilling, such as leakage, overflow, collapsing and sticking, especially when the lost circulation and blowout happen simultaneously in the same open interval, which is very difficult to deal with. These problems seriously restrict the drilling speed.

Maintaining wellbore stability is an important issue in the oil and gas industry. The economic

*Corresponding author, Ph.D., E-mail: yanchuanliang@163.com

loss caused by wellbore instability reaches more than one billion dollar every year (Mohammad 2012), and the lost time accounts for over 40% of all drilling related non-productive time (Dodson *et al.* 2004, Zhang *et al.* 2009). Wells with high down-hole temperature have a higher risk of wellbore instability resulted from temperature changing (Nguyen *et al.* 2015). The research of thermal effect on wellbore stability began in the early 1980s, the temperature of the drilling fluid was considered on designing the construction of geothermal well in former Soviet Union (Li 2004). Maury and Guenot (1995) pointed out that thermal stress is one of the factors leading to wellbore instability. The temperature data around the wellbore with different diameters were measured. It

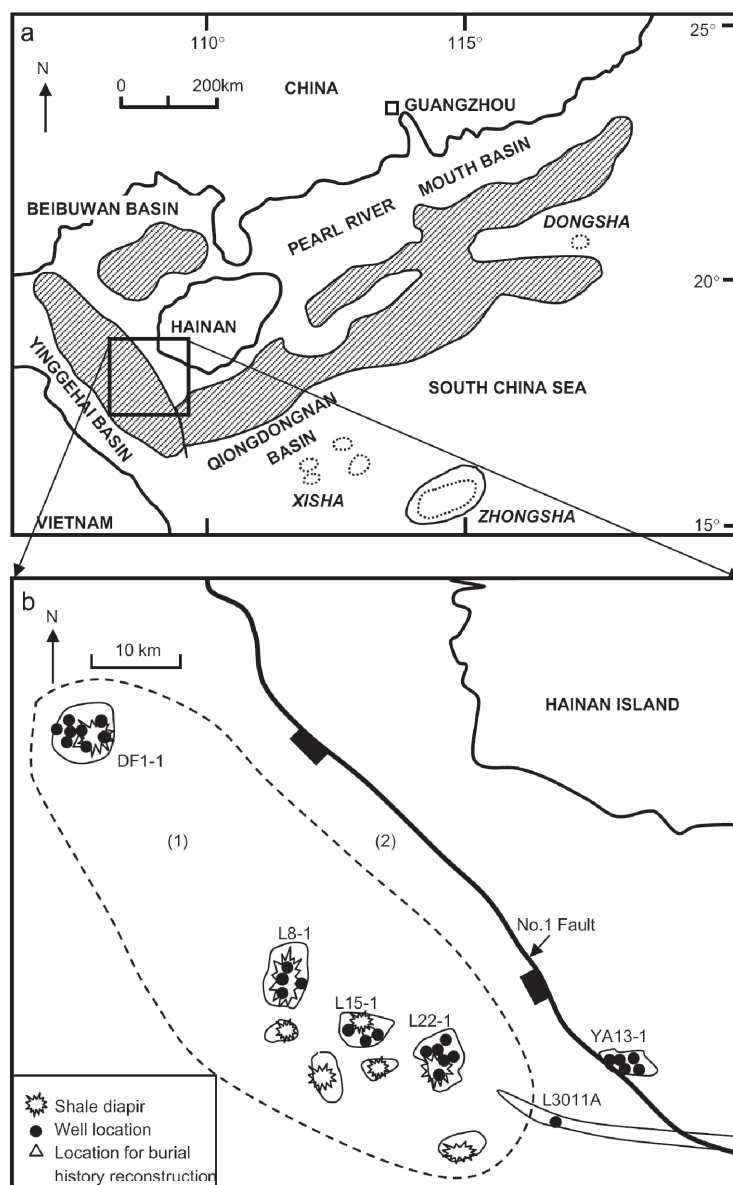


Fig. 1 Location of DF1-1 gas field (Wang and Huang 2008)

was also demonstrated in an experiment that 0.4 MPa thermal stress will be generated with every 1°C increase in temperature for rocks with medium hardness, while 1 MPa for hard rocks. In a deep well, the temperature of wellbore wall changes 50°C or more is quite common (Li *et al.* 2005), which means that it may produce 50 MPa thermal stress. Such large thermal stress should by no means be ignored. Combined effect of such thermal stress and the original stress on the wellbore wall may exceed the rock strength and cause collapse or fracture of the wellbore when circulation occurs in wells at depth of 4,000-5,000 m or the temperature gradient larger than 3.5°C/100m or a vertical open interval more than 1,000 m (Li 2004).

In order to prevent the wellbore instability of high temperature high pressure formation in DF1-1 gas field, this paper established a model which can calculate the temperature field around the wellbore. The effect of temperature change on rock mechanical property was studied by experiments and a wellbore stability model was established which has taken thermal effect into consideration. On this basis, the influence rule of temperature change on safe mud density window was analyzed.

2. Geological history

The DF1-1 gas field, discovered in 1992, is located in the Yinggehai Basin, about 100 km west of Yinggehai town, Hainan province (Fig. 1). The Yinggehai Basin is a northwest-trending transform extension basin, which began to develop in Mesozoic times on the passive continental margin of the northern South China Sea. The basin is delineated by NW–SE trending extensional and trans-tensional faults in the northeast and southwest. The tectonic evolution history of the Yinggehai Basin can be divided into a syn-rift stage and a post-rift thermal subsidence stage (Gong 1997).

The top-down deposition sequences are Quaternary Led-formation, Neogene Yinggh-formation and Neogene Huangl-formation. The lithology is mainly sandstone and shale. Huangl-formation is the main gas reservoir of DF1-1 gas field. According to the twenty wells in use, Huangl-formation is high temperature and high pressure formation and is most prone to wellbore instability. Too low drilling fluid density in Huangl-formation is easy to cause overflow, while too high density leads to mud leakage.

3. Rock mechanical test

3.1 Rock strength

9 rock samples from Yinggh-formation and 9 rock samples from Huangl-formation were tested in the experiment. Testing cores were standardized, diameters 25 mm and slenderness ratio 1.8 to 2.0. The uniaxial and triaxial compressive tests were carried on these samples using MTS-816 Rock Test System as the experimental equipment. Experimental results are shown in Table 1.

Yinggh-formation is soft in strength, while Huangl-formation is medium to hard in strength. Huangl-formation has high strength and small ductility, in which case hard-brittle failure occurs under uniaxial compressive force (Fig. 2(a)). The formation has plasticity under confining pressure (Fig. 2(b)), and its collapsing strength, yield stress and plasticity increase with confining pressure.

3.2 Profiles of rock mechanical parameters

Only parameters at specific location can be tested through experiments. Logging data is the

Table 1 Results of compressive strength test

Formation	Depth (m)	Confining pressure (MPa)	Failure strength (MPa)	Cohesion force (MPa)	Internal friction angle (°)
Yinggh	1271.2	0	9.85	3.32	23.17
		5	22.01		
		10	32.84		
Yinggh	1337.5	0	12.24	4.67	28.48
		5	36.64		
		10	40.45		
Yinggh	1380.3	0	22.39	6.57	25.71
		8	37.85		
		15	60.52		
Huangl	2864.5	0	62.29	16.61	34.13
		15	116.43		
		30	168.84		
Huangl	2985.4	0	59.34	17.48	29.78
		15	106.78		
		30	148.54		
Huangl	3034.3	0	49.6	13.40	35.65
		15	114.32		
		30	163.42		

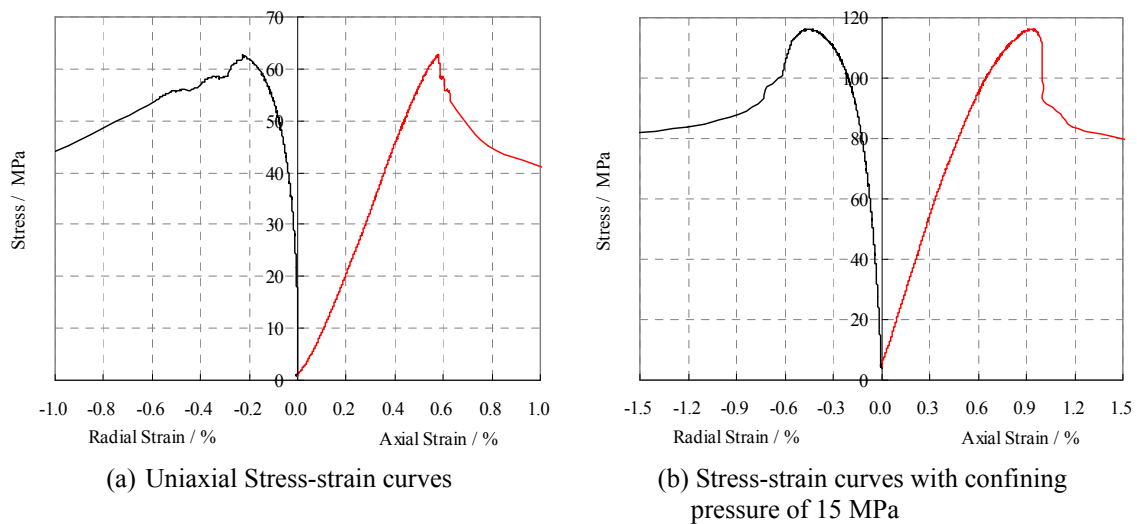


Fig. 2 Stress-strain curves of Huangl-formation

critical element to establish the prediction models and study rock mechanical parameters of the total formation. The commonly used rock mechanics prediction models were chosen and above testing results (Table 1) were used to calibrate the coefficients of the prediction models by the

method of multi-variable linear regression analysis.

The prediction model of uniaxial compressive strength (UCS) can be expressed as (Zhu *et al.* 2012)

$$UCS=f_1E(1-V_{cl})+f_2EV_{cl} \tag{1}$$

Where: E is the Young’s modulus; V_{cl} is the clay mineral content, goes from 0-1; f_1 and f_2 are coefficients. The prediction error of the model is less than 4.7% compared with the experimental results.

Dynamic Young’s modulus and Poisson’s ratio can be calculated by the density of formation, compressive wave velocity and shear wave velocity (Jin *et al.* 2011).

$$\begin{cases} E_d=\rho v_p^2(3v_p^2-4v_s^2)/(v_p^2-2v_s^2) \\ \mu_d=(v_p^2-2v_s^2)/2(v_p^2-2v_s^2) \end{cases} \tag{2}$$

Where, E_d is the dynamic Young’s modulus; μ_d is the dynamic Poisson’s ratio; v_p is the compressive wave velocity; v_s is the shear wave velocity; ρ is the formation density.

The dynamic Young’s modulus and Poisson’s ratio calculated by the acoustic velocity reflect the formation mechanical properties under transient load. However, the load applied to the formation is static. Through the dynamic and static test of rocks synchronously, Lin (*et al.* 1998) obtained the calculation method of static Young’s modulus and static Poisson’s ratio

$$\begin{cases} E_s=0.2526+0.7095E_d(10^4\text{MPa}) \\ \mu_s=0.1268+0.250\mu_d \end{cases} \tag{3}$$

Where: E_s is the static Young’s modulus, 10^4 MPa; μ_s is the static Poisson’s ratio.

The relationships between the cohesion force and UCS were established by Al-Awad (2002).

$$C=-0.417+0.289 \times UCS-0.000519 \times UCS^2 \tag{4}$$

For another strength parameter of internal friction angle, Based on Mohr-Coulomb strength criterion, the internal friction angle can be calculated by UCS and cohesion force

$$\phi=\frac{360}{\pi} \arctan\left(\frac{UCS}{2C}\right)-45 \tag{5}$$

Where, C is the cohesion force; ϕ is the internal friction angle.

By using the rock mechanical parameters prediction model, the profile of rock mechanical parameters of DF1-1 gas field is established (see Fig. 3). The average UCS values of Led-formation, Yinggh-formation and Huangl-formation are 5.97 MPa, 23.09 MPa and 46.86 MPa, respectively. The maximum value of UCS is 77.17 MPa in Huangl-formation and the minimum value of UCS is 2.57 MPa in Led-formation. The strength parameters (UCS, internal friction angle and cohesion force) decrease with the increase of depth at the lower part of Huangl-formation.

3.3 Influence of temperature on formation strength

The UCS of shale and sandstone in DF1-1 gas field were tested at different temperatures. A test

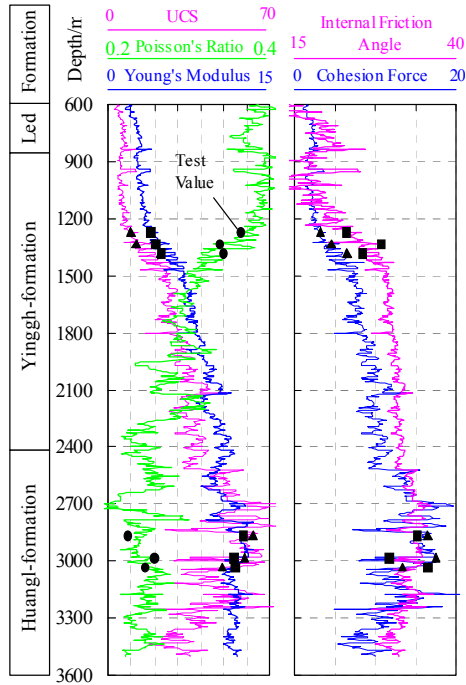


Fig. 3 Profiles of rock mechanical parameters of DF1-1-11 well

Table 2 Rock strength at different temperature

Temperature (°C)	Failure strength (MPa)	
	Shale	Sandstone
25	58.73	65.28
50	52.25	65.95
75	49.38	65.45
100	44.03	67.13
125	40.02	65.46
150	38.76	69.10
175	36.41	68.89
200	34.33	69.48

of acoustic wave velocity was conducted for all cores under the same conditions using the Intelligent Ultrasonic Apparatus of Rock. For the sake of contrastive analysis, core samples of shale and sandstone with similar acoustic velocity were selected, separately. The experimental results are shown in Table 2. The influences of temperature on formation strength are primarily as follows:

- (1) Formation strength of different kinds of rocks respond differently to temperature, the UCS of shale decreases with the increase of temperature and the UCS of sandstone increases slightly.

- (2) The change of Rock strength with temperature can be basically described with the linear law.

$$UCS_c = UCS_{c_0} - K(T - T_0) \tag{6}$$

Where, T is the temperature when the rock strength was measured; T_0 is the room temperature (25°C); UCS_c is the UCS when temperature is T ; UCS_{c_0} is the UCS under room temperature; K is the changing rate of rock strength, which can be determined by experiments.

- (3) The temperature has a significant effect on rock strength. The effect of temperature variation on formation strength must be considered in calculating collapse pressure of a deep well or high geothermal gradient well. Shale is the vulnerable formation most prone to wellbore instability (Zeynali 2012), at the same time temperature has the largest effect on its strength. The influence of temperature should be particularly considered in calculating collapse pressure of shale.

3.4 Thermal expansion coefficient

The thermal expansion coefficient is one of the significant parameters influencing the calculation of stress around a wellbore. In this study, the effect of temperature variations on rock deformation was measured to obtain the thermal expansion coefficient. In the test, only the temperature was variable. The strain recorded in the test was resulted from single action of temperature change and the volumetric strain was exactly the thermal expansion strain. The thermal expansion coefficients of shale and sandstone of Huangl-formation in DF1-1 gas field were tested in this research. The experimental results are shown in Fig. 4. And the thermal expansion coefficients calculated from the experimental results are $\alpha_m = 2.1 \times 10^{-5}$ for shale and $\alpha_m = 1.83 \times 10^{-5}$ for sandstone.

4. Temperature around the wellbore during mud circulation

There are two methods to calculate temperature fields around the wellbore: analytical solution

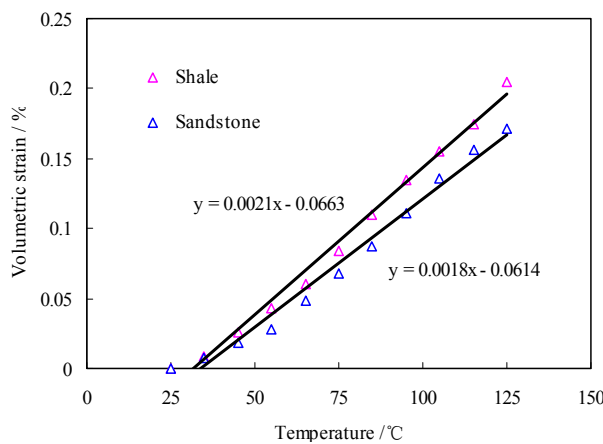


Fig. 4 Thermal strain of rocks

and numerical solution. The analytical solution (Hasan and Kabir 1994) cannot describe the effects of such factors as multiple casing structure, fluid performance parameters etc. on temperature fields around the wellbore due to the fact that the well structure of actual high-temperature wells is usually very complex. The numerical model of down-hole heat transfer has been popularized and applied constantly (Raymond 1969, Espinosa-Paredes *et al.* 2009, Wong-Loya 2012, Yang *et al.* 2013, Llanos *et al.* 2015, Ni *et al.* 2016).

During drilling, the drilling fluid continuously exchanges heat with the formation in the circulation process, specifically manifested by constant variation of drilling fluid temperature and formation temperature. The process of drilling fluid circulating in the wellbore can be divided into three stages.

- (1) The process of drilling fluid entering the drill string from the ground and flowing downward through the drill string.
- (2) The process of drilling fluid entering the annulus from the drill string through drill bit at the bottom. The change in heat energy of the drilling fluid flowing through the drill bit is ignored, temperatures of drilling fluid in the annulus and drill string are the same at the well bottom
- (3) The process of drilling fluid flowing upward in annulus and reaching the ground.

The temperature fields of drilling fluid and formation can be determined by governing Eqs. (7)-(9) and supplementary Eq. (10).

Governing equation in the drill string is as following

$$A_D \rho V_D C_p \frac{\partial T_D(z, t)}{\partial z} + 2\pi r_D U [T_D(z, t) - T_A(z, t)] = -\rho A_D C_p \frac{\partial T_D(z, t)}{\partial t} \quad (7)$$

Governing equation in the annulus is as following

$$A_A \rho V_A C_p \frac{\partial T_A(z, t)}{\partial z} + 2\pi r_D U [T_D(z, t) - T_A(z, t)] + 2\pi r_B h_f [T_f(r_B z, t) - T_A(z, t)] = \rho A_A C_p \frac{\partial T_A(z, t)}{\partial t} \quad (8)$$

Governing equation in the formation is as following

$$\frac{\partial T_f(r, z, t)}{\partial t} = \frac{K_f}{\rho_f C_{pf}} \frac{1}{r} \frac{\partial}{\partial r} \left[r \frac{\partial T_f(r, z, t)}{\partial r} \right] \quad (9)$$

Supplementary equation on the wellbore wall is

$$2\pi r_B h_f [T_f(Z, t) - T_A(Z, t)] = 2\pi r_B K_f \left[\frac{\partial T_f(Z, t)}{\partial r} \right]_{r=r_B} \quad (10)$$

Boundary conditions and initial conditions are described by Eqs. (11)-(14). The inlet temperature of the drilling fluid is known.

$$T_D(Z=0, t) = T_{D0}(t) \quad (11)$$

At the well bottom, the temperature of fluid in the drill string and annulus are identical.

$$T_D(Z = L, t) = T_A(Z = L, t) \tag{12}$$

At an infinite distance of the formation, the temperature is equal to the initial temperature in the same depth.

$$T_f(r_\infty, Z, t) = T_\infty(Z) \tag{13}$$

At the initial time, the temperature in and around wellbore is equal to the original formation temperature.

$$T_D(Z, 0) = T_A(Z, 0) = T_f(r, Z, 0) = T_\infty(Z) \tag{14}$$

Where, T_D , T_A and T_f are temperatures of fluid in the drill string, annulus fluid temperature and formation temperature, respectively; A_D and A_A are cross sectional areas of the drill string and the annulus, respectively; V_D and V_A are flow velocities of fluid in the drill string and annulus, respectively; ρ and ρ_f are circulating fluid density and formation density, respectively; C_p and C_{pf} are specific heat of circulating fluid and formation, respectively; r_D and r_B are radius of drill string and wellbore, respectively; K_f is the heat conduction coefficient of formation; h_f is the coefficient of heat convection of wellbore wall; U is the coefficient of overall heat convection of fluid–solid interface; $T_\infty(Z)$ is the original temperature of formation and is a function of depth and geothermal gradient; t is mud circulating time.

5. Wellbore stability model with thermal effect

5.1 Wellbore stability of vertical wells

Based on the thermoelasticity theory, the additional thermal stress around the wellbore resulted from temperature variation can be described as follows

$$\begin{cases} \sigma_{rT} = \frac{E\alpha_m}{3(1-\nu)} \frac{1}{r^2} \int_{r_w}^r T^f(r, t) r dr \\ \sigma_{\theta T} = \frac{E\alpha_m}{3(1-\nu)} \left[T^f(r, t) - \frac{1}{r^2} \int_{r_w}^r T^f(r, t) r dr \right] \\ \sigma_{zT} = \frac{E\alpha_m}{3(1-\nu)} T^f(r, t) \end{cases} \tag{15}$$

Where, σ_{rT} , $\sigma_{\theta T}$ and σ_{zT} are additional radial stress, additional tangential stress and additional axial stress around the wellbore resulted from thermal effect, respectively; $T^f(r, t) = T(r, t) - T_0$, is the temperature variation field of formation around the well; E is the Young’s modulus; ν is the Poisson’s ratio.

Many published literatures have provided the method of calculating the stress around the wellbore under the effects of in-situ stress and column pressure of drilling fluid (Al-Ajmi and Zimmerman 2006, Fjær *et al.* 2008). On this basis, using the superposition principle, the stress

around the wellbore with thermal effect considered can be described as follows

$$\left\{ \begin{array}{l} \sigma_r = \frac{r_B^2}{r^2} P_w + \frac{\sigma_H + \sigma_h}{2} \left(1 - \frac{r_B^2}{r^2} \right) + \frac{\sigma_H - \sigma_h}{2} \left(1 + 3 \frac{r_B^4}{r^4} - 4 \frac{r_B^2}{r^2} \right) \cos 2\theta + \delta \left[\xi \left(1 - \frac{r_B^2}{r^2} \right) - f \right] (P_w - P_p) \\ \quad + \frac{E\alpha_m}{3(1-\nu)} \frac{1}{r^2} \int_{r_B}^r T^f(r,t) r dr \\ \sigma_\theta = -\frac{r_B^2}{r^2} P_w + \frac{\sigma_H + \sigma_h}{2} \left(1 + \frac{r_B^2}{r^2} \right) - \frac{\sigma_H - \sigma_h}{2} \left(1 + 3 \frac{r_B^4}{r^4} \right) \cos 2\theta + \delta \left[\xi \left(1 + \frac{r_B^2}{r^2} \right) - f \right] (P_w - P_p) \\ \quad + \frac{E\alpha_m}{3(1-\nu)} \left[\frac{1}{r^2} \int_{r_B}^r T^f(r,t) r dr - T^f(r,t) \right] \\ \sigma_z = \sigma_v - \nu \left[2(\sigma_H - \sigma_h) \frac{r_B^2}{r^2} \cos 2\theta \right] + \delta(2\xi - f)(P_w - P_p) + \frac{E\alpha_m}{3(1-\nu)} T^f(r,t) \end{array} \right. \quad (16)$$

Where, σ_r , σ_θ and σ_z are radial stress, tangential stress and axial stress around the wellbore; σ_v , σ_H and σ_h are overburden stress, maximum horizontal stress and minimum horizontal stress respectively; P_w is the mud pressure in wellbore; P_p is the pore pressure; $\xi = \alpha(1-2\nu)/(2(1-\nu))$; α is the Biot's coefficient; f is the formation porosity; θ is the angle from the direction of σ_H to the radius vector of the point near the wellbore; δ is the seepage coefficient of wellbore wall, $\delta = 0$ if there is no seepage and $\delta = 1$ if seepage happens.

Shear failure of the wellbore is subject to the Mohr-Coulomb strength criterion. Shear failure will occur when the Mohr's circle constituted by the maximum and minimum effective principal stress on the wellbore wall exceeds the failure strength. The Mohr-Coulomb strength criterion expressed by principal stress is as following (Sofianos and Nomikos 2006)

$$(\sigma_1 - \alpha P_p) = (\sigma_3 - \alpha P_p) \tan^2 \left(\frac{\pi}{4} + \frac{\varphi}{2} \right) + 2C \tan \left(\frac{\pi}{4} + \frac{\varphi}{2} \right) \quad (17)$$

Where, σ_1 and σ_3 are the maximum and minimum principal stress.

The collapse pressure with thermal effect taken into account is

$$P_{cr} = \frac{3\sigma_H - \sigma_h - 2CK + [\delta\zeta + \delta f K^2 + \alpha(1 + K^2)(1 - \delta)]P_p + E\alpha_m(T_w - T_0)/[3(1 - \nu)]}{1 - \delta\zeta + \alpha\delta + K^2(1 - \delta f - \alpha\delta)} \quad (18)$$

Where, $K = \tan(\pi/4 + \varphi/2)$; $\zeta = \alpha(1 - 2\nu)/(1 - \nu) - f$.

Fracture occurs when the tangential effective stress on the wellbore wall reaches the tensile strength of rock (Fjær *et al.* 2008).

$$\sigma_\theta - \alpha P_p = -St \quad (19)$$

The fracture pressure with the thermal effect taken into account is

$$P_f = \frac{3(1 - \nu)[3\sigma_h - \sigma_H + St - (\delta\zeta + \alpha - \alpha\delta)P_p] + E\alpha_m(T_w - T_0)}{3(1 + \alpha\delta - \delta\zeta)(1 - \nu)} \quad (20)$$

5.2 Wellbore stability of directional well

Assuming the formation as homogeneous and isotropic porous elastic material, the stress around a directional well can be got (Jin *et al.* 1999). Based on the superposition principle in combination of this basis, the stress around a directional well with thermal effect considered is as follows

$$\left\{ \begin{aligned}
 \sigma_r &= \frac{R^2}{r^2} P_w + \frac{(\sigma_{xx} + \sigma_{yy})}{2} \left(1 - \frac{R^2}{r^2}\right) + \frac{(\sigma_{xx} - \sigma_{yy})}{2} \left(1 + \frac{3R^4}{r^4} - \frac{4R^2}{r^2}\right) \cos 2\theta + \sigma_{xy} \left(1 + \frac{3R^4}{r^4} - \frac{4R^2}{r^2}\right) \sin 2\theta \\
 &+ \delta \left[\xi \left(1 - \frac{r_B^2}{r^2}\right) - f \right] (P_w - P_p) + \frac{E\alpha_m}{3(1-\nu)} \frac{1}{r^2} \int_{r_B}^r T^f(r,t) r dr \\
 \sigma_\theta &= -\frac{R^2}{r^2} P_w + \frac{(\sigma_{xx} + \sigma_{yy})}{2} \left(1 + \frac{R^2}{r^2}\right) - \frac{(\sigma_{xx} - \sigma_{yy})}{2} \left(1 + \frac{3R^4}{r^4}\right) \cos 2\theta - \sigma_{xy} \left(1 + \frac{3R^4}{r^4} - \frac{4R^2}{r^2}\right) \sin 2\theta + \\
 &\delta \left[\xi \left(1 + \frac{r_B^2}{r^2}\right) - f \right] (P_w - P_p) + \frac{E\alpha_m}{3(1-\nu)} \left[\frac{1}{r^2} \int_{r_B}^r T^f(r,t) r dr - T^f(r,t) \right] \\
 \sigma_z &= \sigma_{zz} - \nu [2(\sigma_{xx} - \sigma_{yy}) \left(\frac{R}{r}\right)^2 \cos 2\theta + 4\sigma_{xy} \left(\frac{R}{r}\right)^2 \sin 2\theta] \sigma_\nu + \delta (2\xi - f) (P_w - P_p) + \frac{E\alpha_m}{3(1-\nu)} T^f(r,t) \\
 \sigma_{r\theta} &= \sigma_{xy} \left(1 - \frac{3R^4}{r^4} + \frac{2R^2}{r^2}\right) \cos 2\theta \\
 \sigma_{\theta z} &= \sigma_{yz} \left(1 + \frac{R^2}{r^2}\right) \cos \theta - \sigma_{xz} \left(1 + \frac{R^2}{r^2}\right) \sin \theta \\
 \sigma_{zr} &= \sigma_{xz} \left(1 - \frac{R^2}{r^2}\right) \cos \theta + \sigma_{yz} \left(1 - \frac{R^2}{r^2}\right) \sin \theta
 \end{aligned} \right. \quad (21)$$

Where σ with the subscript r, θ, z are the normal stress and shear stress in cylindrical coordinates; σ with subscript x, y, z are the normal stress and shear stress in Descartes coordinates; R is the radius to hole axis, r is the wellbore radius; θ is the azimuth relative to the x -axis. Transformation from the in-situ stress to stress in Descartes coordinates can be obtained through coordinate conversion (Jin *et al.* 1999).

Under elastic state, the maximum stress concentration appears on the wellbore wall, the principal stress on the wellbore wall is as follows

$$\sigma_{t\max} / \sigma_{t\min} = \frac{(\sigma_\theta + \sigma_z)}{2} \pm \sqrt{\left(\frac{\sigma_\theta - \sigma_z}{2}\right)^2 + \sigma_{\theta z}^2} \quad (22)$$

Where, $\sigma_{t\max}$ and $\sigma_{t\min}$ is the principal stress. Radial stress of σ_r is another principal stress. The relative magnitude of the three principal stresses change with the density of drilling fluid. The maximum and minimum principal stresses with any drilling fluid density is

$$\begin{cases} \sigma_1 = \max(\sigma_{t\max}, \sigma_{t\min}, \sigma_r) \\ \sigma_3 = \min(\sigma_{t\max}, \sigma_{t\min}, \sigma_r) \end{cases} \quad (23)$$

Insert Eq. (23) into Eq. (17), and then the collapse pressure of directional well can be got. The

fracture pressure of directional well is determined by Eq. (24) (Zhu *et al.* 2015)

$$\sigma_3 - \alpha P_p = -St \tag{24}$$

6. Wellbore stability analysis in DF1-1 gas field

The maximum horizontal stress direction of DF1-1 gas field is N165°E. Figs. 5 and 6 are collapse pressure and fracture pressure of Huangl-formation in DF1-1 gas field. The collapse pressure and fracture pressure of a vertical well are 1.7 g/cm³ and 2.28 g/cm³ respectively. The collapse pressure of horizontal well is between 1.77 g/cm³ and 1.79 g/cm³ and the fracture pressure

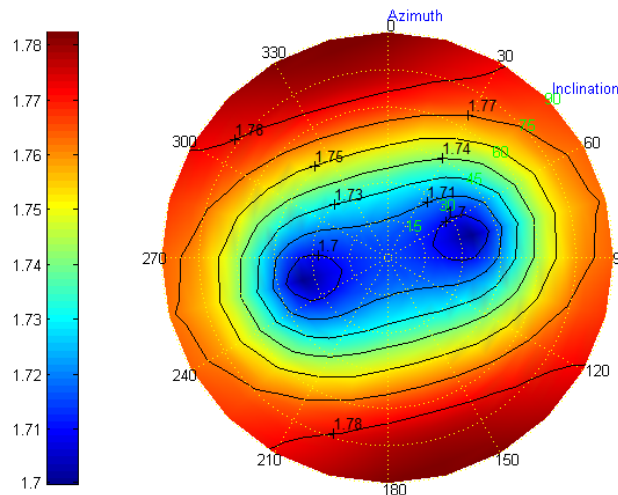


Fig. 5 Collapse pressure of directional wells versus well track

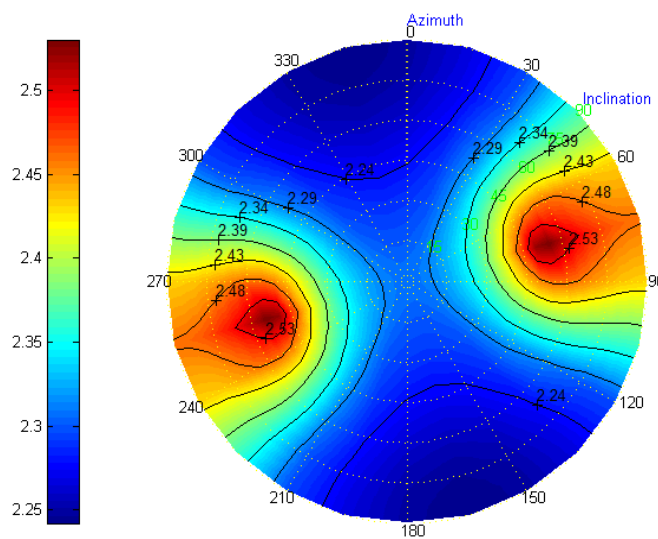


Fig. 6 Fracture pressure of directional wells versus well track

of horizontal well is between 2.19 g/cm^3 and 2.48 g/cm^3 . The risk of wellbore instability is the highest when drilling toward the maximum horizontal stress direction with the highest collapse pressure and lowest fracture pressure. The risk of wellbore instability is the lowest when drilling toward the minimum horizontal stress direction.

The temperature field of DF1-1-11 well during mud circulation is analyzed. This is a vertical well with a total depth of 3500 m.

The parameters used in calculation are as follows:

Parameters of drilling fluid: density = 2.1 g/cm^3 , specific heat = $3.44 \text{ J/(g}\cdot\text{°C)}$, coefficient of heat conduction = $0.62 \text{ W/(m}\cdot\text{°C)}$, consistency index = $0.051 \text{ Pa}\cdot\text{S}^n$, rheology index = 0.94, mud displacement = 32-40 L/s.

Formation parameters: density = 2.5 g/cm^3 , specific heat = $0.84 \text{ J/(g}\cdot\text{°C)}$, coefficient of heat conduction = $3.42 \text{ W/(m}\cdot\text{°C)}$.

Steel parameters: coefficient of heat conduction = $53.60 \text{ W/(m}\cdot\text{°C)}$; specific heat = $0.465 \text{ J/(g}\cdot\text{°C)}$.

Fig. 7 shows the variation regularity of wellbore wall temperature during mud circulation. During drilling, the drilling fluid will exchange heat with the formation which leads to the

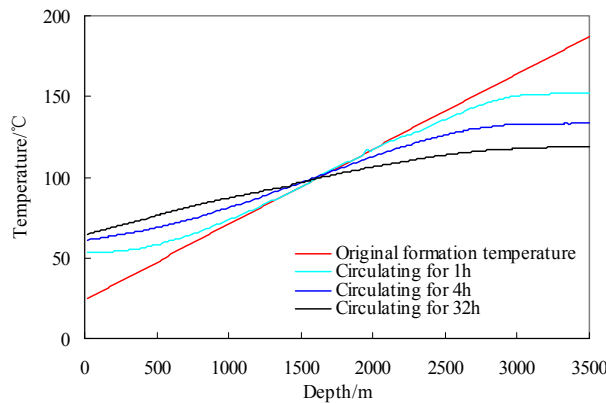


Fig. 7 Variation of wellbore wall temperature with well depth and circulation time

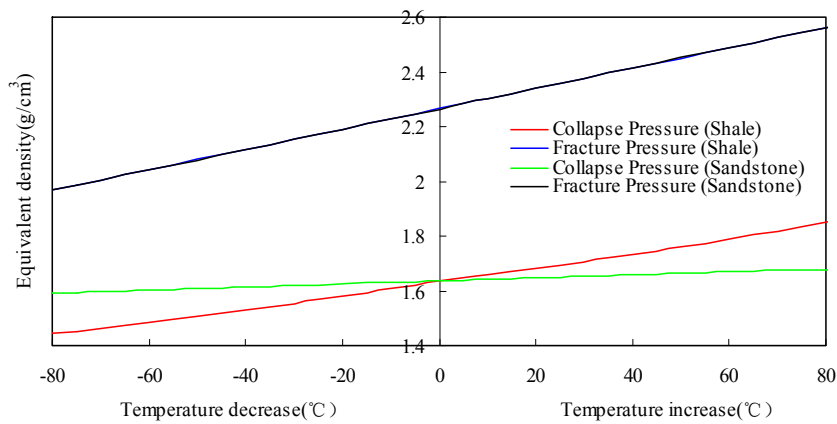


Fig. 8 Effect of temperature changing on collapse pressure and fracture pressure

decrease of temperature of lower formation and increase of temperature of upper formation; the location in certain depth with constant formation temperature is referred to as the “neutral point”; the temperature of wellbore wall in the well sections below the neutral point falls and the temperature above the neutral point rises; the neutral point rises with the circulation time. The changing rate of temperature decreases with circulation time. The temperature will approach a certain constant value and temperature will not be subject to circulation after a period of circulation.

Assume the variation of formation tensile strength with temperature is the same with UCS, the influence of temperature increase and temperature decrease on safe drilling fluid density is shown in Fig. 8. The fracture pressure and collapse pressure both increased with the wellbore temperature increase, but the increasing rate of collapse pressure is smaller than the fracture pressure, so the safe mud density window will widen. The fracture pressure and collapse pressure both decreased with the wellbore temperature decrease, but the decreasing rate of collapse is smaller than the fracture pressure, so the safe mud density window will narrow.

The shale strength strongly depends on the temperature, so the temperature has larger effect on the collapse pressure of shale than that of sandstone. Since fracture pressure is mainly affected by the stress around the wellbore, lithology has little effect on the fracture pressure which varies with temperature.

Fig. 9 shows the collapse pressure and fracture pressure of DF1-1-11 well varying with depth and circulation time. The safe mud density window between pore pressure and fracture pressure in

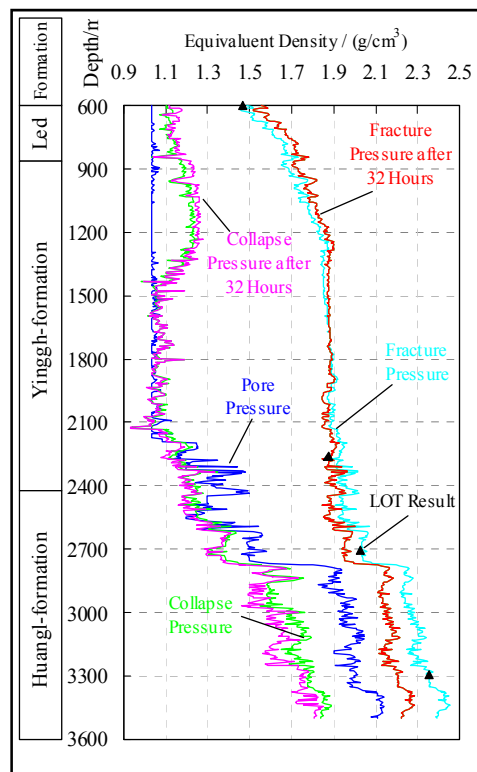


Fig. 9 Safe mud density window of DF1-1-11 Well

Huangl-formation is very narrow with no more than 0.3 g/cm^3 when the hole is just drilled open. Before Huangl-formation the safe mud density window is wide. Affected by the drilling fluid circulation, the temperature of Huangl-formation decreased and the fracture pressure reduced significantly. Compared with the result without consideration of thermal effect, with 32 hours circulation, the maximum reduction of fracture pressure is about 0.17 g/cm^3 at the hole bottom with 32 hours circulation. Thus, it is necessary to take thermal effect into account when drilling in high temperature and high pressure formation. The collapse pressure of shale reduces in Huangl-formation with the circulation time, but sandstone changes little. The temperature of upper formation will increase under the effect of drilling fluid circulation, but it should be noted that the collapse pressure of upper formation before 1500 m increases with drilling time. Thermal effect may lead to the risk increase of wellbore collapse in the upper formation, especially in shale. When drilling long open intervals, it is necessary to take extra care of thermal effect on collapse pressure of shale in upper formation. In Huangl-formation, the collapse pressure is lower than the pore pressure. As a result, formation collapse is not the main challenge, but the more important thing is to prevent overflow and mud leakage. After a period of circulation, even if the circulation time increases, the temperature of wellbore is basically not changed, the collapse pressure and fracture pressure remain at a constant value.

7. Conclusions

As the heat exchange between the drilling fluid and formation, the temperature of lower formation decreases and the temperature of upper formation increases. The maximum change of temperature is on the wellbore wall and then gradually decreases from internal to the formation.

The UCS of shale decreases with the increase of temperature while sandstone strength increases slightly. Temperature rise will make the formation expansion and swelling stress can be produced. When the temperature decreases, the collapse pressure and fracture pressure are both decreased. At this time, reducing the density of drilling fluid properly can prevent mud leakage. When the temperature rises, the collapse pressure and fracture pressure are both increased. Especially in shale formation, the strength significantly reduces with the increase of temperature, which also exacerbates the increase of collapse pressure, in which case, increase the drilling fluid density properly can help to prevent collapse. The effect of temperature variation on fracture pressure is larger than that on the collapse pressure, but variation of fracture pressure is not related to lithology.

The safe mud density window of Huangl-formation in DF1-1 gas field is narrow. As a result, overflow and mud leakage are the biggest problems in drilling. After drilling, the temperature reduction will further reduce the fracture pressure, which will increase the risk of mud leakage. More attention should be paid on preventing drilling fluid leakage after drilling.

Drilling in the formation with high temperature and high pressure, the predictive precision of safe drilling fluid density should be significantly improved when taking thermal effect into consideration.

High temperature high pressure is very common in many oil and gas fields in South China Sea, and the problems of drilling in these fields are similar. The research results of DF1-1 gas field can provide a reference for these fields.

Acknowledgments

This work is financially supported by the Changjiang Scholars and Innovative Research Team in University (Grant No. IRT_14R58), National Basic Research Program of China (973 Program) (Grant No. 2015CB251201), National key research and development program (Grant No. 2016YFC0304005), the National Natural Science Foundation Project of China (Grant No. 51504280, 51504040), Fundamental Research Funds for the Central Universities (Grant No. 15CX02009A), Qingdao Science and Technology Project (Grant No. 15-9-1-55-jch).

References

- Al-Ajmi, A.M. and Zimmerman, R.W. (2006), "Stability analysis of vertical boreholes using the Mogi–Coulomb failure criterion", *Int. J. Rock Mech. Min. Sci.*, **43**, 1200-1211.
- Al-Awad, M.N. (2002), "Simple correlation to evaluate Mohr-Coulomb failure criterion using uniaxial compressive strength", *J. King Saud Univ.*, **14**(1), 137-145.
- Dodson, J., Dodson, T. and Schmidt, V. (2004), "Gulf of Mexico 'trouble time' creates major drilling expenses: Use of cost-effective technologies needed", *Offshore*, **64**(1), 46-48.
- Espinosa-Paredes, G., Morales-Díaz, A., Olea-González, U. and Ambriz-García, J.J. (2009), "Application of a proportional-integral control for the estimation of static formation temperatures in oil wells", *Mar. Petrol. Geol.*, **26**(2), 259-268.
- Fjær, E., Holt, R.M., Horsrud, P., Raaen, A.M. and Risnes, R. (2008), *Petroleum Related Rock Mechanics*, (Second Edition), Elsevier.
- Gong, Z.S. (1997), *The Major Offshore Oil and Gas Fields in China*, Petroleum Industry Press, Beijing, China.
- Hasan, A.R. and Kabir, C.S. (1994), "Static reservoir temperature determination from transient data after mud circulation", *SPE Drill. Completion*, **9**(1), 7-24.
- Jiang, P., He, W. and Cheng, T. (2012), "Practices of economic and high-effective development in the Dongfang 1-1 Gas Field, Yinggehai Basin", *Nat. Gas Ind.*, **32**(8), 16-21.
- Jin, Y., Chen, M. and Liu, G.H. (1999), "Wellbore stability analysis of extended reach wells", *J. Geomech.*, **5**(1), 4-11.
- Jin, Y., Yuan, J., Chen, M., Chen, K.P., Lu, Y. and Wang, H. (2011), "Determination of Rock Fracture Toughness K_{IIC} and its Relationship with Tensile Strength", *Rock Mech. Rock Eng.*, **44**(5), 621-627.
- Li, S.G. (2004), "The Study on HT/HP Wellbore Stability", Ph.D. Dissertation; China University of Petroleum.
- Li, S.G., Deng, J.G., Yu, B.H. and Yu, L.J. (2005), "Formation fracture pressure calculation in high temperatures wells", *China J. Rock Mech. Eng.*, **24**(S2), 5669-5673.
- Lin, Y.S., Ge, H.K. and Wang, S.C. (1998), "Testing study on dynamic and static elastic parameters of rocks", *China J. Rock Mech. Eng.*, **17**(2), 216-222.
- Llanos, E.M., Zarrouk, S.J. and Hogarth, R.A. (2015), "Numerical model of the Habanero geothermal reservoir, Australia", *Geothermics*, **53**, 308-319.
- Maurly, V. and Guenot, A. (1995), "Practical advantages of mud cooling systems for drilling", *SPE Drill. Completion*, **10**(1), 42-48.
- Mohammad, E.Z. (2012), "Mechanical and physical-chemical aspects of wellbore stability during drilling operations", *J. Pet. Sci. Eng.*, **82-83**, 120-124.
- Nguyen, S.T., Hoang, S.K., Khuc, G.H. and Tran, H.N. (2015), "Pore pressure and fracture gradient prediction for the challenging high pressure and high temperature well, Hai Thach Field, Block 05-2, Nam Con Son Basin, Offshore Vietnam: A case study", *SPE/IATMI Asia Pacific Oil & Gas Conference and Exhibition*, Nusa Dua, Bali, Indonesia, October.
- Ni, H., Song, W., Wang, R. and Shen, Z. (2016), "Coupling model for carbon dioxide wellbore flow and

- heat transfer in coiled tubing drilling”, *J. Nat. Gas Sci. Eng.*, **30**, 414-420.
- Raymond, L.R. (1969), “Temperature distribution in a circulating drilling fluid”, *J. Pet. Technol.*, **21**(3), 333-341.
- Sofianos, A.I. and Nomikos, P.P. (2006), “Equivalent Mohr–Coulomb and generalized Hoek–Brown strength parameters for supported axisymmetric tunnels in plastic or brittle rock”, *Int. J. Rock Mech. Min. Sci.*, **43**(5), 683-704.
- Wang, Z.F. and Huang, B.J. (2008), “Dongfang 1-1 gas field in the mud diapir belt of the Yinggehai Basin, South China Sea”, *Mar. Petrol. Geol.*, **25**(4), 445-455.
- Wong-Loya, J.A., Andaverde, J. and Santoyo, E. (2012), “A new practical method for the determination of static formation temperatures in geothermal and petroleum wells using a numerical method based on rational polynomial functions”, *J. Geophys. Eng.*, **9**(6), 711-723.
- Yang, M., Meng, Y.F., Li, G., Deng, J.M. and Zhao, X.Y. (2013), “A transient heat transfer model of wellbore and formation during the whole drilling process”, *Acta Petrolei Sinica*, **34**(2), 366-371.
- Zeynali, M.E. (2012), “Mechanical and physico-chemical aspects of wellbore stability during drilling operations”, *J. Pet. Sci. Eng.*, **82**, 120-124.
- Zhang, J.C., Lang, J. and Standifird, W. (2009), “Stress, porosity, and failure-dependent compressional and shear velocity ratio and its application to wellbore stability”, *J. Pet. Sci. Eng.*, **69**, 193-202.
- Zhu, H.Y., Deng, J.G., Xie, Y.H., Huang, K.W., Zhao, J.Y. and Yu, B.H. (2012), “Rock mechanics characteristic of complex formation and faster drilling techniques in Western South China Sea oilfields”, *Ocean Eng.*, **44**, 33-45.
- Zhu, H.Y., Deng, J.G. and Huang, K.W. (2013), “Characteristics of rock mechanics and PDC bit optimization of glutenite formation in the Pearl River Mouth Basin oilfields”, *Sci Iran Trans A: Civ Eng.*, **20**(4), 1133-1144.
- Zhu, H.Y., Guo J.C., Zhao, X., Lu, Q., Luo, B. and Feng, Y.C. (2014), “Hydraulic fracture initiation pressure of anisotropic shale gas reservoirs”, *Geomech. Eng., Int. J.*, **7**(4), 403-430.
- Zhu, H.Y., Zhang X.D. and Guo J.C. (2015), “Stress field interference of hydraulic fractures in layered formation”, *Geomech. Eng., Int. J.*, **9**(5), 645-667.